

## **Processes of Soil Erosion by Wind**

**L. J. Hagen**

Wind Erosion Research Unit, USDA, ARS,  
Kansas State University, 2004 Throckmorton  
Plant Sciences Center, Manhattan, KS 66506

---

Contribution from USDA, ARS in cooperation with Kansas Agricultural Experiment Station,  
Contribution No. \_\_\_\_\_

**Abstract** In the past, wind erosion has often been modeled as a series of lumped factors, and each factor embodied a number of individual erosion processes. During the last decade considerable progress has been made in formulating process equations that represent the individual sources and sinks for eroding soil. The objective of this report is to provide an overview of some wind erosion processes on agricultural lands. By considering two soil states (crusted and aggregated) along with the erosion processes, one can define the temporal soil properties of dry soils that control soil erodibility. These temporal properties include the dry stabilities, mass fractions and size distributions of mobile and immobile soil components, as well as surface roughness. The threshold friction velocities of bare soils also depend upon surface roughness and cover of immobile clods and crusts. The transport capacity of the suspension-size soil is several times larger than the limited transport capacity for the saltation and creep-size component of horizontal soil discharge. Thus, on large fields suspension discharge often exceeds saltation/creep discharge. Sources of saltation/creep discharge include entrainment of loose aggregates and abrasion of immobile clods and crust. Sinks for saltation/creep discharge include trapping by surface roughness, interception by standing biomass and breakage to suspension-size. Similarly, sources for suspension discharge include entrainment of loose aggregates, abrasion of clods and crust, and breakage of saltation/creep aggregates. Sinks for suspension include interception by standing biomass and deposition on downwind immobile surfaces. Wind tunnels have been used to measure directly the parameters for the individual wind erosion processes. Moreover, the individual processes can be assembled into physically-based wind erosion models that are applicable to a wide range of surface conditions.

**keywords:** Wind erosion, erosion processes, particulate, dust, soil, PM10, PM2.5.

The early work of Bagnold (1941) provided a firm basis toward understanding the processes involved with wind transport of loose, dry sand. Among the processes he studied were effects of wind and particle interactions on threshold velocities and horizontal mass transport rates. Subsequent research on erosion mechanics of loose particles has expanded upon Bagnold's initial work (Anderson, et al.,1991). However, complex wind patterns and surface wetness still make predicting the transport of sand on dunes and on beaches a challenging research area (Van Dijk et al.1999; White and Tsoar, 1998; Gares, 1988 ).

Animal and human impacts on agricultural lands in semi-arid and arid areas have often accelerated natural wind erosion. As a result, there has been considerable research aimed at predicting and controlling wind erosion on these lands (Chepil and Woodruff, 1963; Leys, 1999). However, agricultural land surfaces are often more complex than bare, dry, loose sands. For complex agricultural surfaces, researchers identified the major factors that influenced wind erosion. But the need to convey erosion prediction and controls in simplified models, lead researchers to further lump the factors. These lumped factors included effects of soil erodibility, climate, surface roughness, field scale, and vegetation ( Woodruff and Siddoway, 1965; Fryrear et al., 1998).

In general, the lumped factors contain a number of wind erosion processes that obscure interactions among the processes and often require calibration to field measurements before application (Saxton et al., 2000 ). The widespread availability of computers now makes it feasible to consider individual processes in wind erosion prediction and control systems. As a result, several recent models of wind erosion have been oriented toward simulating individual erosion processes in desert lands (Marticorena and Bergametti, 1995; Draxler et al., 2001) and on

agricultural lands (Shao, et al., 1996; Hagen, 1999 ). This approach has two attractive features: first, individual processes can be defined to facilitate experimental parameter development in wind tunnels without the requirement for field calibration (Hagen, 2001c; Mirzamostafa et. al., 1998). Second, the processes can readily be combined to build complex models applicable to a wide range of surface conditions (Hagen et al., 1999). Of course, field validation of models is still a much-needed part of comprehensive wind erosion research programs.

The purpose of this report is to provide an overview of wind erosion processes on agricultural lands. In this endeavor, we shall provide only brief comments on well-known results and focus on some of the lesser-known, but nevertheless important, processes associated with wind erosion. Areas that need additional research also will be briefly discussed.

### **Soil Surface Conditions**

To facilitate understanding of erosion processes, it is useful to consider two general states of the soil surface. The surface may be composed of loose aggregates as exemplified by a newly-tilled surface. But the most common surface condition consists of an upper layer with a water-consolidated zone that has a partial cover of loose, mobile aggregates. These loose aggregates are often sand grains or water stable aggregates that are a result of raindrop impacts (Chepil and Woodruff, 1963 ). However, the loose aggregates may be absent from a crust created by snowmelt on the same soil. For this discussion, we shall refer to the entire water-consolidated zone as crust, although crust usually is defined as only the densest, upper portion of the consolidated zone. Obviously, strip tillage or other processes may create surfaces where both states are present. Crusted surfaces without a source of mobile aggregates to serve as abrader are

generally stable, except under extreme winds (Marticorena et al., 1997). Similarly, surfaces composed of loose, immobile aggregates may be stable.

Although efforts have been made to classify wind erodibility of various soils (Chepil and Woodruff, 1963), the precision of the classification has been hampered because, as yet, there is not an accepted standard measurement for it. Some of the difficulties in defining a standard measure results from the fact that for a defined wind storm, the upwind and downwind ends of a field generally are subjected to different amounts of abrasion by saltating aggregates. Thus, locations on the same field have differing soil losses. Moreover, the soil conditions that control erodibility are temporal and depend upon both soil management and weather. However, by considering the erosion processes and the soil state, one can define measurable, temporal, soil parameters that control soil wind erodibility (Table 1). Using validated erosion models to integrate the effects of the temporal soil parameters on soil loss over time may prove to be the most efficient method to classify wind erodibility of soils.

Table 1. Temporal soil parameters that control wind erodibility of dry, bare soil.

Parameters	Soil State	
	Crusted with loose cover	Loose aggregates
Dry aggregate stability by layer:		
Mobile	X	X
Immobile	X	X
Roughness:		
Random	X	X
Oriented	X	X
Crusted:		
Loose mass on top	X	
Crust (consolidated zone) thickness	X	
Aggregate size distribution by layer:		
All soil layers		X
Layers below crust	X	
Rock fraction (>2 mm) by layer	X	X

The dry stability of immobile crusts and clods can be measured by crushing energy meters (Boyd et. al., 1983; Hagen et.al.; 1995). The range of the temporal distribution of the crushing energy also has been related to soil clay content (Skidmore and Layton, 1992). Stability of mobile, saltation-size aggregates is approximately nine times that of the immobile clods of the same soil as measured by impact breakage tests on a small number of soils (Mirzamostafa, et al., 1998). In the past, repeated sieving has been used as an clod stability indicator (Chepil and Woodruff, 1963). However, in tests (unpublished) we found that repeated sieving generally destroyed weak aggregates with a crushing energy  $< 0.5$  J/kg, but was largely insensitive to the stability range of stronger aggregates.

Medium-textured, crusted soils generally have lower wind erodibilities than similar uncrusted soils, but the dry stability of the crust is usually equal or less than that of the underlying clods (Chepil and Woodruff, 1963; Zobeck and Popham, 1992) . Thus, the reduction in erodibility of crusted soils is likely caused by lower amounts of available mobile soil on the crust than among loose, surface aggregates. Loose soil on crusts can be sampled using vacuum devices (Zobeck, 1989), wind tunnels, or even a soft brush and pan. Relationships to predict the loose materials on crusts have been developed for a few soils (Potter, 1990).

In contrast, the reduction in roughness caused by rainfall or irrigation on sandy soils (Zobeck and Onstad, 1987) often leave them more erodible than their aggregated, pre-rain condition. Hence, rolling tined cultivators (“sand fighters”) are often used after rain on these soils to restore some of the random roughness and shelter the mobile aggregates from the wind.

While wind erosion is a surface phenomenon, measurement of parameters in several soil

layers is suggested, so that one can estimate the effects of soil disturbance. For example, disturbance of a desert pavement typically creates a highly erodible surface. In contrast, emergency tillage of crop land is often used to roughen and bring clods to the surface to reduce soil erodibility.

When estimating average soil erosion, it is important to determine the distribution of the soil temporal conditions, because, in general, amount of soil erosion is non-linearly related to the surface soil conditions as illustrated by the example in Fig. 1. Thus, if one uses the mean surface condition, 0.5, to estimate average relative erosion, the result is  $Y1 = 0.11$ . However, if the surface conditions have a normal distribution ( mean = 0.5 , standard deviation = 0.15), then average erosion is  $Y2 = 0.14$ . Finally, if surface conditions have a uniform distribution, the average relative erosion would be  $Y3 = 0.22$ . When the wind speed distribution is also included in simulations, the non-linearity of erosion response to surface conditions increases further (Hagen, 1996). One may readily conclude from this example, that inputting only average soil conditions in erosion models may estimate erosion for the average soil condition, but may not estimate that which the model user may be seeking, namely, average erosion. Overall, additional research is needed to improve the understanding, distributions, and predictions of the soil temporal properties that control wind erosion.

### **Threshold friction velocities**

The wind shearing stress or drag ( $\tau$ ) on the soil surface is related to the friction velocity ( $u_*$ ) as

$$\tau = \rho(u_*)^2 \quad (1)$$

where  $\rho$  is air density. Early experimental data demonstrated that the static threshold friction velocity ( $u_{*t}$ ) where particle movement on a smooth bed of erodible particles began depended on both particle diameter and density, as well as air density (Bagnold, 1941). Moreover, once erosion began on a surface with an unlimited source of particles, it would continue until the velocity was reduced below a dynamic threshold friction velocity which was about  $0.8 u_{*t}$ . Later measurements showed that interparticle cohesive force increased the  $u_{*t}$  of small particles and gravitational force increased  $u_{*t}$  of large particles above a minimum  $u_{*t}$  which occurred for particle beds with diameters ranging from about 60 to 100  $\mu\text{m}$  (Chepil, 1958; Iversen and White, 1982).

On erodible surfaces with a partial cover of uniformly distributed non-erodible elements, measurements show drag on the surface is split between the protruding elements and the intervening erodible surface (Marshall, 1971; Lyles et al., 1974). Frontal area of the protruding elements is the major variable controlling the drag partitioning. For this case, Raupach (1992) proposed an analytical formula that gave reasonable agreement with the measurements. However, it is not feasible to determine frontal area on a bare soil surface with random distribution of both the non-erodible aggregates and surface heights. To overcome this difficulty, Marticorena and Bergamette (1995) proposed that

$$u_{*t}(D_p, Z_o, Z_{os}) = \frac{u_{*ts}(D_p)}{b(Z_o, Z_{os})} \quad (2)$$

where  $D_p$  is the diameter of the erodible particles, and  $Z_o$  is the aerodynamic surface roughness.

The threshold friction velocity on a smooth bed ( $u_{*c}$ ), and the aerodynamic roughness ( $Z_{os}$ ) are functions of  $D_p$ . The fractional values of the efficiency factor ( $b$ ) were estimated using the empirical equation

$$b = 1 - \frac{\ln(Z/Z_{os})}{\ln[0.35(10/Z_{os})^{0.8}]} \quad (3)$$

The values of  $b$  were highly correlated with the measured data of Marshall (1971) and Raupach (1992) on surfaces with a narrow size range of erodible particles and uniform protruding non-erodible elements.

But there remain a number of difficulties in applying the preceding two equations to agricultural fields. The macro-roughness that determines  $Z_o$  is usually initiated by tillage and then modified by weathering forces (Zobeck and Onstad, 1987). Unfortunately, the macro-roughness is generally not correlated with the aggregate size distribution (Wagner and Hagen, 1991). Thus, the surface fraction covered by immobile soil aggregates or crust is not represented in the preceding equation. Obviously, there is a significant difference in threshold velocities between tillage ridges normal to the wind direction that are composed of mobile particles and the same ridge stabilized by a crust with a few mobile particles in the shelter between the ridges. The value to choose for  $D_p$  is also uncertain for soils with a distribution of erodible aggregate sizes. Draxler et al. (2001) slightly modified the equation to calculate  $b$  and further suggested that  $D_p$  should be assigned the mean soil aggregate diameter.

Currently, the WEPS erosion submodel (Hagen, et al., 1999) uses an empirical family of curves to estimate  $u_{*c}$  on dry, bare, mineral soil of the form (Fig. 2)

$$u_{*t} = f(Z_o, F_c), \quad F_c < 1.0 \quad (4)$$

where  $F_c$  is fraction surface cover of immobile clods and crust  $> 0.84$  mm diameter. Minimum  $u_{*t}$  is set at  $0.24 \text{ m s}^{-1}$ .

Other factors also increase surface threshold velocities. Measurements show surface wetness (Saleh and Fryrear, 1995; McKenna-Nueman and Nickling, 1989) begins to increase threshold velocity at soil water contents well below plant wilting point. Flat and standing biomass increase threshold velocities as well as interact with the mobile soil aggregates (Hagen, 1996, Armbrust and Bilbro, 1997; Retta et al., 1996).

### **Wind Erosion Transport Modes and Capacities**

There are three modes of wind erosion transport. Creep-size aggregates (0.8 - 2.0 mm in diameter) roll along the surface in intermittent motion propelled by both wind gusts and saltation impacts. Saltation-size aggregates (0.1 - 0.8 mm in diameter) saltate (hop) along the surface, while suspension-size ( $< 0.1$  mm in diameter) generally move above the surface with little surface contact. Obviously, the size limits in a given transport mode vary somewhat depending upon wind speed and aggregate density.

It is useful to delineate between transport capacity for saltation/creep-size aggregates and suspension-size. Accurate horizontal mass discharge data for saltation and creep are difficult to obtain, and a variety of equations have been derived (Greeley and Iversen, 1985). One of the most frequently used was developed by Lettau and Lettau (1978) and can be expressed as

$$q_{en} = C_s u_*^2 (u_* - u_{*t}) \quad (5)$$

where  $C_s$  is the saltation transport parameter ( $\text{kg m}^{-4} \text{s}^2$ ), with a typical value of about 0.3 or more for surfaces armored with stones,  $u_*$  is friction velocity ( $\text{m s}^{-1}$ ), and  $u_{*c}$  is dynamic threshold friction velocity ( $\text{m s}^{-1}$ ). A maximum discharge from a smooth field ( aerodynamic roughness 0.003 m) with friction velocity equal  $0.74 \text{ m s}^{-1}$  (wind speed equal  $15 \text{ m s}^{-1}$  at 10 m height) would be  $0.08 \text{ kg m}^{-1} \text{ s}^{-1}$ . As surface roughness and shelter by immobile cover increases,  $u_{*c}$  also increases resulting in lower transport capacities for saltation and creep-size aggregates. When the immobile shelter is sufficient to prevent incoming saltation from impacting mobile aggregates, measurements show  $u_{*c}$  increases from the dynamic to static threshold (Hagen and Armbrust, 1992).

In contrast to the limited transport capacity for saltation/creep, the transport capacity for suspension is much larger and can be considered nearly unlimited on typical eroding fields. To illustrate, consider the following example based on concentration and visibility measurements in a series of dust storms (Chepil and Woodruff, 1957 ). The average concentration,  $C_o$  ( $\text{mg m}^{-3}$ ) at 1.83 m as a function of visibility,  $V$  (km) was measured as

$$C_o = \frac{56}{V^{1.25}} \quad (6)$$

The average vertical concentration profile,  $C(z)$  followed a power law, and can be represented as

$$C(z) = C_o \left( \frac{z}{1.83} \right)^{0.28} \quad (7)$$

The suspension discharge,  $q_{ss}$  ( $\text{kg m}^{-1} \text{ s}^{-1}$ ), for any visibility can then be estimated as

$$q_{ss} = \int_{z_0}^{z_1} C(0.1) u(z) dz + \int_{z_1}^{z_2} C(z) u(z) dz \quad (8)$$

For this example, the wind speed was  $15 \text{ m s}^{-1}$  at 10 m height, while  $u(z)$  represented the log-law vertical wind speed profile. The dust concentration was uniform in the active saltation zone extending from  $z_0$  to 0.1 m, and the slope of the diffusion zone was estimated as 1:50 so that  $z_2$  was 16 m and 32 m at 800 and 1600 m downwind, respectively. The example results show that as visibility is reduced below about 0.5 km, one can expect the suspension transport to exceed the maximum saltation and creep transport (Fig. 3). Moreover, at low visibilities where vehicle traffic is impeded, suspension transport greatly exceeds the saltation and creep transport from a single field.

### Saltation and Creep Discharge

In this section, we shall consider the individual processes that control the saltation/creep discharge. Based on conservation of mass in a control volume (Fig. 4), a one-dimensional, quasi-steady state equation for the physical processes involved in saltation/creep is:

$$\frac{dq}{dx} = G_{en} + G_{an} - G_{ssbk} - G_{tp} \quad (9)$$

where  $q$  is horizontal saltation/creep discharge ( $\text{kg m}^{-1} \text{ s}^{-1}$ ),  $x$  is downwind distance from non-erodible boundary (m),  $G_{en}$  is vertical flux from emission of loose aggregates ( $\text{kg m}^{-2} \text{ s}^{-1}$ ),  $G_{an}$  is vertical flux from abrasion of surface clods and crust ( $\text{kg m}^{-2} \text{ s}^{-1}$ ),  $G_{ssbk}$  is vertical flux of

suspension aggregates from breakage of saltation/creep aggregates ( $\text{kg m}^{-2} \text{s}^{-1}$ ), and  $G_{t,p}$  is vertical flux from trapping of saltation/creep aggregates ( $\text{kg m}^{-2} \text{s}^{-1}$ ).

Each of the vertical fluxes represents either source or sink terms in the control volume and can be estimated by the equations that follow.

The net emission source term for loose aggregates is

$$G_{en} = (1 - SF_{ss_{en}}) C_{en} (q_{en} - q) \quad (10)$$

where  $SF_{ss_{en}}$  is mass fraction of suspension-size ( $< 0.10$  mm) among loose aggregates ( $< 2.0$  mm diameter),  $C_{en}$  is coefficient of emission ( $\text{m}^{-1}$ ), and  $q_{en}$  is transport capacity ( $\text{kg m}^{-1} \text{s}^{-1}$ ).

A typical value for  $C_{en}$  on a loose, bare field is about  $0.06 \text{ m}^{-1}$ , and values for other conditions have been reported (Hagen, 1995). At transport capacity,  $dq/dx$  equals zero. However, the emission and/or abrasion flux must still continue over the entire field to satisfy the discharge lost to breakage and/or trapping. In this case, the actual transport capacity must be some value of  $q$  that is less than  $q_{en}$ .

The suspension-size aggregates are assumed to be mixed intimately with the saltation/creep-size and emitted with them. Although the suspension-size aggregates absorb part of the aerodynamic and impact energy (represented by the emission coefficient) in order to rise from the surface, they do not contribute toward reaching the transport capacity of saltation/creep. Hence, they are subtracted from the total emission of loose aggregates in Eq.10.

The net source term for entrainment of saltation/creep aggregates abraded from immobile clods and crust by impacting saltation/creep is

$$G_{an} = (1 - SF_{ss_{an}}) \left[ \sum_1^2 (F_{ani} C_{ani}) q \right] \left( \frac{q_{en} - q}{q_{en}} \right) \quad (11)$$

where  $SF_{ss_{an}}$  is mass fraction of suspension-size from abrasion,  $F_{ani}$  is mass fraction saltation impacting clods and crust, and  $C_{ani}$  is coefficient of abrasion ( $m^{-1}$ ).

An index of two was used in Eq. 11 because, in general, only two targets, exposed clods and crust, must be considered. Other targets, such as residue and rocks, have a  $C_{ani}$  near zero. The first term,  $(1 - SF_{ss_{an}})$ , is the fraction of abraded mass that is of saltation/creep-size. Values of  $SF_{ss_{an}}$  for some Kansas soils have been measured and ranged from 0.14 to 0.27, depending upon soil texture (Mirzamostafa, 1996). The middle, bracketed term on the right-hand-side of Eq. 11 represents the total soil abraded from clods and crust, as confirmed by wind tunnel experiments (Hagen, 1991). Values for  $C_{ani}$  also have been measured for a range of soils and related to clod crushing energy (Fig. 5, Hagen, et al., 1992). The final term in Eq. 11 is the mass fraction entrained in the air stream. The entrainment rate of this newly-created saltation/creep is assumed to be similar to that of loose, saltation/creep-size aggregates already present on the surface, and that the entrainment approaches zero at transport capacity.

A sink for the saltation/creep discharge occurs when these aggregates are broken into suspension-size and carried away by convection and diffusion (Mirzamostafa, et al., 1998). This effect is simulated as

$$G_{ssbk} = C_{bk} (q - q_s) \quad (12)$$

where  $C_{bk}$  is coefficient of breakage ( $m^{-1}$ ), and  $q_s$  is discharge of primary (non-breakable) sand particles ( $kg\ m^{-1}\ s^{-1}$ ).

The saltation/creep aggregates are more stable than the surface clods and crust, so measured abrasion coefficients average about nine times more than the breakage coefficients on the same soils (Mirzamostafa, 1996). The wind tunnel experiments also demonstrated that the breakage coefficient remained constant during breakdown of the aggregates to primary particles. The means and variances of these coefficients are related to soil texture. Given  $q$ , values for  $q_s$  can be estimated directly from soil sand content

Another sink term is the removal of saltation/creep from the air stream by trapping mechanisms (Hagen and Armbrust, 1992). Surface trapping and plant interception can be simulated as

$$G_{tp} = C_t \left(1 - \frac{q_{cp}}{q_{en}}\right) q + C_i q \quad (13)$$

where  $C_t$  is coefficient of surface trapping ( $m^{-1}$ ),  $C_i$  is coefficient of plant interception ( $m^{-1}$ ), and  $q_{cp}$  is transport capacity of the surface, when 40 percent or more is armored ( $kg\ m^{-1}\ s^{-1}$ ).

When erosive winds cross rough surfaces, such as tillage ridges, that are highly erodible, large amounts of soil are entrained, but a portion of the entrained saltation/creep is often trapped in succeeding downwind furrows. This phenomenon results in a local rearrangement of the surface and reduces net removal of the entrained soil. Our conventionally-defined transport capacity,  $q_{en}$ , is based on the threshold velocity where erosion begins. But, when trapping of saltation/creep occurs on rough surfaces, one may hypothesize that  $q_{en}$  has been exceeded, and

that the true transport capacity of the surface is some value,  $q_{cp}$ , that is less than  $q_{en}$ . However,  $q_{en}$  still appears to be the appropriate limiting value to drive the emission process, because more soil is emitted than can be transported from the local area.

Thus, the first term on the right-hand-side of Eq. 13 simulates trapping of saltation/creep by surface roughness. The true transport capacity of the surface,  $q_{cp}$ , is based on the threshold friction velocity needed to remove saltation/creep from the furrows. It is calculated using threshold friction velocity for a given roughness at the level of clod and crust cover of the surface but with a minimum set at 40 percent of the surface armored. Under this condition, wind tunnel observations show that loose material is removed, but minimal local trapping of saltation/creep occurs.

The second term of Eq. 13 represents interception of saltation/creep by standing plant stalks or other near-surface plant parts. This term arises, because for a given soil surface friction velocity, more transport occurs without than with stalks. This term also is used to assign a higher transport capacity for wind direction parallel to crop rows than for wind direction perpendicular to rows. For saltation normal to the row direction, interception can reduce transport capacity 5 to 10 percent or more. Comparisons to measured data have been reported previously (Hagen and Armbrust, 1994).

### **Suspension Discharge**

Based on conservation of mass in a control volume that extends to the top of the dust cloud, a one-dimensional, quasi-steady state equation for the physical processes generating the suspension component is

$$\frac{dq_{ss}}{dx} = G_{ss_{en}} + G_{ss_{an}} + G_{ss_{bk}} - G_{ss_{tp}}, \quad u_* > u_{*t} \quad (14)$$

or

$$\frac{dq_{ss}}{dx} = G_{SS_{dp}}, \quad u_* < u_{*t} \quad (15)$$

where  $q_{ss}$  is horizontal suspension component discharge ( $\text{kg m}^{-1} \text{s}^{-1}$ ),  $G_{ss_{en}}$  is vertical emission flux of loose, suspension-size aggregates ( $\text{kg m}^{-2} \text{s}^{-1}$ ),  $G_{ss_{an}}$  is vertical flux of suspension-size aggregates created by abrasion of clods and crust ( $\text{kg m}^{-2} \text{s}^{-1}$ ),  $G_{ss_{bk}}$  is vertical flux of suspension-size aggregates created by breakage of saltation/creep-size aggregates ( $\text{kg m}^{-2} \text{s}^{-1}$ ),  $G_{ss_{tp}}$  is vertical flux from trapping suspension-size aggregates, and  $G_{SS_{dp}}$  is vertical flux (deposition) of suspension-size aggregates above a non-eroding surface ( $\text{kg m}^{-2} \text{s}^{-1}$ ).

The source and sink terms for the suspension component can be simulated by the equations that follow.

For direct emission of loose, suspension-size material by 'splash' impacts and aerodynamic forces

$$G_{ss_{en}} = SF_{ss_{en}} C_{en} (q_{en} - q) + C_m q \quad (16)$$

where  $C_m$  is a coefficient of mixing, value about  $(0.0001 SF_{ss_{en}}) (\text{m}^{-1})$ .

Below transport capacity, the driving force causing the emission flux of suspension-size soil is assumed to be similar to that in Eq. 10 causing the saltation/creep emission flux. This assumption is supported by wind tunnel measurements that show a mixture of suspension-size aggregates and a mixture of saltation-size have about the same threshold velocities (Chepil,

1951).

However, two additional assumptions are inherent in Eq. 16 . The first is that the loose components of saltation/creep and suspension-size aggregates occur as a uniform mixture in the field. As a consequence, during simple net emission, the suspension fraction emitted with the saltation/creep remains the same as it was in the soil. Hence, the suspension fraction can be estimated as

$$SF_{ss_{en}} = \frac{SF_{ss}}{SF_{er}} \quad (17)$$

where  $SF_{ss}$  is soil mass fraction of loose, suspension-size less than about 0.1 mm, and  $SF_{er}$  is soil mass fraction of loose, erodible-size, less than about 2.0 mm.

The second assumption in Eq. 16 is that an additional small amount of suspension-size aggregates that are disturbed by the saltation impacts also are entrained, because transport capacity for the suspension component generally is not limiting. The result of this process is gradual depletion of the loose, suspension-size aggregates at the surface. However, when net emission of suspension-size exceeds net emission of saltation/creep-size aggregates, the latter soon dominate the surface area and absorb the impacts, so the process tends to be self-limiting.

For suspension flux created by abrasion of clods and crust,

$$G_{ss_{an}} = SF_{ss_{an}} \sum_1^2 (F_{ani} C_{ani}) q \quad (18)$$

Additional discussion and measurements of this source term were reported by Mirzamostafa et

al.,1998.

For the source of suspension flux created by breakage of saltation/creep aggregates, the term is the same as the sink term in the saltation/creep equation and simulated as

$$G_{ss_{bk}} = C_{bk}(q - q_s) \quad (19)$$

Breakage from impact on immovable targets is assumed to come only from the impacting saltation/creep alone. Breakage coefficients for saltation-size aggregates have been measured in the wind tunnel (Mizamostafa et al.,1998). But the breakage component from impacts on other saltation/creep is assumed to come from both the impacting and target aggregates. Breakage from impact on a mobile target is less likely than breakage from impact on immobile targets. However, these assumptions need further experimental verification.

When exiting the biomass canopy, a small portion of the suspension component also maybe trapped or intercepted by plants similar to interception of saltation/creep. This effect likely is relatively small in the sparse biomass populations that permit erosion. Nevertheless, additional experimental data are needed to quantify this process.

Another, sink term for trapping of suspension flux occurs when the suspension discharge passes over areas without active saltation to maintain the suspension flux from the surface. Typically, this implies the presence of a vegetated, water, or rough armored surface. The largest suspension particles, 0.05 to 0.10 mm, comprise roughly half the mass of the suspension discharge (Chepil, 1957; Zobeck and Fryrear, 1986). Through diffusion and settling, they move rapidly toward non-eroding surfaces in the simulation region, which serve as sinks. The process is simulated as

$$G_{ss_{dp}} = C_{dp}(q_{ss} - q_{ss_o}), \quad q_{ss} > 0.5q_{ss_o} \quad (20)$$

where  $q_{ss_0}$  is maximum value of  $q_{ss}$  entering deposition region ( $\text{kg m}^{-1} \text{s}^{-1}$ ), and  $C_{dp}$  is coefficient of deposition of suspension-size ( $\text{m}^{-1}$ ). The maximum value of  $C_{dp}$  is about 0.02, but less for smooth surfaces or large upwind areas that produce high dust clouds thus, moving a large portion of the soil away from the deposition surface. Others have shown the deposition flux is a function of surface roughness, surface retention characteristics, and particle size (Schack et al., 1985; Reynolds, 2000). Thus, the preceding equation is only a rough approximation of near-field deposition. Additional research is needed to provide predicted concentration profiles and size distributions of suspension-size soil that occur over the range of wind-erodible soils.

As illustrated by the preceding equations, generation of the suspension component is intimately associated with the saltation/creep component. Analytic solutions for these linked saltation/creep and suspension discharge differential equations have been developed (Hagen et al., 1999) and validated using measured data from small fields (Hagen, 2201a). The suspension component has a large transport capacity, and the suspension generation processes occur over the entire eroding area. Thus, on uniform, eroding areas one would expect that suspension discharge should continually increase in the downwind direction. Data collected at Owens Lake in California illustrates nicely the differing response of saltation/creep and suspension discharge on a large area (Fig. 6, Gillette et al., 1997). In these data, the saltation/creep transport capacity occurs at about 660 m downwind, while there is a continual increase in the suspension discharge in the downwind direction. Although only a portion of the suspension component was collected in the samplers, it still greatly exceeded the saltation/creep transport capacity at 1600 m downwind.

## PM10 and PM2.5 Discharge

Particulate matter with aerodynamic diameters less than 10  $\mu\text{m}$  (PM10) and less than 2.5  $\mu\text{m}$  (PM2.5) are considered health hazards in the United States (Ostro and Chestnut, 1998). Substantial amounts of these fine particles are generated during wind erosion, and high PM10 concentrations cause some locations to be in non-compliance with clean air act standards (Claiborn et al., 2000). PM10 and PM2.5 are generated by the same processes as the other suspension-size particles, so the process equations discussed in the prior section also can be applied to generation of fine PM particles, but with different parameters. Parameters for their simulation have been measured for some soils (Hagen et al., 1996; Hagen and James, 1998; Hagen, 2001b).

New, proposed regulations would require PM2.5 concentrations to be about one-third that of PM10 concentrations (U.S. EPA, 1996). During wind erosion, the highest ratio of PM2.5/PM10 is produced by the breakage process (Hagen and James, 1998). For a range of soils subjected to breakage, the ratio averaged 0.154, but increased with saltation-size sand/clay ratio of the parent soils (Fig. 7, Hagen, 2001b). The PM2.5/PM10 ratio also was inversely related to the annual precipitation (100 - 800 mm range) at sampling sites in the western U.S. Using both sand/clay ratio and annual precipitation in a regression equation gave a coefficient of determination,  $R^2$ , equal 0.53. These data suggest that the proposed PM2.5 standard should not be more difficult to attain than the PM10 standard, when local wind erosion is the only PM2.5 source affecting the target population.

## Conclusions

In prior decades, wind erosion prediction and the design of control measures on agricultural lands often depended on using a series of lumped factors. The lumped factors usually embodied several individual erosion processes. Hence, wind tunnel measurements of factor values that were directly applicable to the field were often problematic. However, during the last decade considerable progress has been made in formulating equations to represent individual erosion processes that constitute the sources and sinks for eroding soil. The soil state and the individual erosion processes can be used to delineate measurable, soil, temporal properties that control wind erosion.

Both the wind erosion processes and their boundary conditions are physically-based and most can be measured individually in wind tunnels. Boundary conditions for the processes include, threshold friction velocities and transport capacity of saltation/creep. Sources of saltation/creep discharge include entrainment of loose aggregates and abrasion of immobile clods and crust. Sinks for saltation/creep discharge include trapping by surface roughness, interception by standing biomass and breakage to suspension-size. Similarly, sources for suspension discharge include entrainment of loose aggregates, abrasion of clods and crust, and breakage of saltation/creep aggregates. Sinks for suspension include interception by standing biomass and deposition on downwind immobile surfaces.

Recently, the individual processes have been assembled into linked differential equations that can estimate erosion for a wide range of surface conditions. This linking allows one to explore the interactions among the various erosion processes. The erosion generated by the individual processes has also been partitioned to the separate transport modes of saltation/creep

and suspension. Current research has begun to delineate the PM10 and PM2.5 generation potential of various soils. Separating the soil discharge leaving a field by direction and into components of saltation/creep, suspension, PM10 and PM2.5 can greatly enhance utility of model predictions for estimating off-site erosion impacts.

## References

- Anderson, R.S., Sorenson, M. and Willets, B.B. 1991. A review of recent progress in our understanding of aeolian sediment transport. *Acta Mechanica (Supplement)* 1:1-19.
- Armbrust, D.V. and Bilbro, J.D. 1997. Relating plant canopy characteristics to soil transport capacity by wind. *Agronomy Journal*. 89(2):157-162.
- Bagnold, R.A. 1941. *The Physics of Blown Sand and Desert Dunes*. Methuen, New York, 265 p.
- Boyd, D.W. , Skidmore, E.L., and Thompson, J.G. 1983. A soil-aggregate crushing-energy meter. *Soil Science Society of America Journal* 47(2):313-316.
- Chepil, W.S. 1951. Properties of soil which influence wind erosion. IV. State of dry aggregate structure. *Soil Science* 75(2):387-401.
- Chepil, W.S. 1957. Sedimentary characteristics of duststorms: III.. Composition of the suspended dust. *American Journal of Science* 255:206-213.
- Chepil, W.S. 1958. Soil conditions that influence wind erosion. Technical Bul. No. 1185, 40 pp., USDA, Washington, D.C.
- Chepil, W.S. and Woodruff, N.P. 1957. Sedimentary characteristics of dust storms: II. Visibility and dust concentration. *American Journal of Science* 255:104-114.
- Chepil, W.S. and N.P. Woodruff. 1963. The physics of wind erosion and its control. *Advances in Agronomy*, 15: 211-302. Academic Press, New York.
- Clairborn, C.S., Finn, D., Larson, T.V., and Koenig, J.Q. 2000. Windblown dust contributes to high PM2.5 concentrations. *Journal of Air & Waste Management Association* 50:1440-1445.
- Draxler, R.R., Gillette, D.A., Kirkpatrick, J.S., and Heller, J. 2001. Estimating PM10 concentrations from dust storms in Iraq, Kuwait, and Saudi Arabia. *Atmospheric Environment* 35:4315 - 4330.
- Fryrear, D.W., Saleh, A. and Bilbro, J.D. 1998. A single event erosion model. *Transactions of the American Society of Agricultural Engineers* 34(1):155-160.
- Gares, P.A. 1988. Factors affecting eolian sediment transport in beach and dune environments. *Journal of Coastal Research, Special Issue* 3:121-126.

- Gillette, D.A., Fryrear, D.W. Xiao, J.B. Stockton, P., Ono, D., Helm, P.J., Gill, T.E. and Ley, T. 1997. Large-scale variability of wind erosion mass flux rates at Owens Lake. 1. Vertical profiles of horizontal mass fluxes of wind-eroded particles with diameter greater than 50  $\mu\text{m}$ . *Journal of Geophysical Research* 102(D22):25,977-25,987.
- Greeley, R. and Iversen, J.D. 1985. *Wind as a Geological Process on Earth, Mars, Venus, and Titan*. Cambridge University Press, New York, 333 p.
- Hagen, L.J. 1991. Wind erosion mechanics: Abrasion of aggregated soil. *Transactions of the American Society of Agricultural Engineers* 34(4):831-837.
- Hagen, L.J. 1995. Erosion submodel. In: *Wind Erosion Prediction System Technical Description*. Proc. of WEPP/WEPS Symposium pp. E1-E47, August 9-11, Des Moines, IA. Soil and Water Conservation Society, Ankeny, IA.
- Hagen, L.J. 1996. Crop residue effects on aerodynamic processes and wind erosion. *Theoretical and Applied Climatology* 54:39-46.
- Hagen, L.J. 1999. Wind Erosion Prediction System: Erosion Submodel. In *Wind Erosion - An International Symposium/Workshop*, E.L. Skidmore and J. Tatarko (Editors), June 3-5, 1997, USDA, ARS, Wind Erosion Research Unit, Kansas State University, Manhattan, KS.
- Hagen, L.J. 2001a. Validation of the Wind Erosion Prediction System (WEPS) erosion submodel on small cropland fields. *Proceedings of International Symposium on Soil Erosion Research for the 21<sup>st</sup> Century*, pp. 479- 482. American Society of Agricultural Engineers, Jan 3-5, Honolulu, Hawaii.
- Hagen, L.J. 2001b. Fine particulates (PM10 and PM2.5) generated by breakage of mobile aggregates during simulated wind erosion. *American Society of Agricultural Engineers Meeting Paper No. 01-2072*, St. Joseph, MI
- Hagen, L.J. 2001c. Assessment of wind erosion parameters using wind tunnels. *Proc. of 10<sup>th</sup> International Soil Conservation Organization Conference*, May 23-28, 1999, Purdue Univ., West Lafayette, IN (in press)
- Hagen, L.J. and Armbrust, D.V. 1992. Aerodynamic roughness and saltation trapping efficiency of tillage ridges. *Transactions of the American Society of Agricultural Engineers* 35(5):1179-1184.
- Hagen, L.J. and Armbrust, D.V. 1994. Plant canopy effects on wind erosion saltation. *Transactions of the American Society of Agricultural Engineers* 37(2):461- 465.

- Hagen, L.J. and James, D.E. 1998. The PM-10 production potential of soils in the Las Vegas Valley of Nevada. In *Dust, Aerosols, Loess Soils and Global Change*,. Busaca, A.J. (Editor), Washington State Univ. College of Agriculture and Home Economics, pp. 45-48. Miscellaneous Pub. No. MISC0190, Pullman, WA.
- Hagen, L.J., Mirzamostafa, N., and Hawkins, A. 1996. PM-10 generation by wind erosion. *International Conference on Air Pollution from Agricultural Operations*, pp.79-86. Feb. 7 - 9, Kansas City, MO.
- Hagen, L.J., Schroeder, B., and Skidmore, E.L. 1995. A vertical soil crushing-energy meter. *Transactions of the American Society of Agricultural Engineers* 38(3):711-715.
- Hagen, L.J., Skidmore, E.L., and Saleh, A. 1992. Wind erosion: prediction of aggregate abrasion coefficients. *Transactions of the American Society of Agricultural Engineers* 35(6):1847-1850.
- Hagen, L.J., Wagner, L.E., and Skidmore, E.L. 1999. Analytical solutions and sensitivity analyses for sediment transport in WEPS. *Transactions of the American Society of Agricultural Engineers* 42(6):1715-1721.
- Iversen, J.D. and White, B.R. 1982. Saltation threshold on Earth, Mars, and Venus. *Sedimentology* 29:111-119.
- Lettau, K. and Lettau, H.H. 1978. Experimental and micro-meteorological field studies of dune migration. In *Exploring the World's Driest Climate*, H.H. Lettau and K. Lettau (Editors), pp. 110-147. Institute for Environmental Studies, IES Report 101, University of Wisconsin-Madison, WI.
- Leys, J. 1999. Wind erosion on agricultural land. In *Aeolian Environments, Sediments, and Landforms*, A.S..Goudie, I. Livingstone, and S. Stokes (Editors), pp.143-166. John Wiley & Sons, New York..
- Lyles, L., Schrandt, R.L., and Schmeidler, N.F. 1974. How aerodynamic roughness elements control sand movement. *Trans. Am. Soc. Agric. Engin.* 17(1):134-139.
- Marshall, J.K. 1971. Drag measurements on roughness arrays of varying density and distribution. *Agric. Meteorol.* 8:269-292.
- Marticorena, B. and Bergametti, G. 1995. Modeling the atmospheric dust cycle: 1. Design of a soil-derived dust emission scheme. *Journal of Geophysical Research* 100(D8):16,415 - 16,430.

- Marticorena, B., Bergametti, G., Gillette, D.A., and Belnap, J. 1997. Factors controlling threshold friction velocity in semiarid and arid areas of the United States. *Journal of Geophysical Research*. 102 (D19): 23,277-23,287.
- McKenna-Neuman, C. and Nickling, W.G. 1989. A theoretical and wind tunnel investigation of the effect of capillary water on the entrainment of sediment by wind. *Canadian Journal of soil science* 69:79-96.
- Mirzamostafa, N. 1996. Suspension component of wind erosion. Ph.D. dissertation, Kansas State University, Manhattan, KS, 126 p.
- Mirzamostafa, N., Hagen, L.J., Stone, L.R., and Skidmore, E.L. 1998. Soil and aggregate texture effects on suspension components from wind erosion. *Soil Science Society of America Journal* 62:1351-1361.
- Ostro, B. and Chestnut, L. 1998. Assessing the health benefits of reducing particulate matter air pollution in the United States. *Environmental Research* 76:94-106.
- Raupach, M.R. 1992. Drag and drag partition on rough surfaces. *Boundary Layer Meteorology*. 60:375-395
- Retta, A., Armbrust, D.V., and Hagen, L.J. 1996. Partitioning biomass in the crop submodel of WEPS (Wind Erosion Prediction System). *Transactions of the American Society of Agricultural Engineers* 39(1):145-151.
- Reynolds, A.M. 2000. Prediction of particle deposition on to rough surfaces. *Agricultural and Forest Meteorology* 104:107-118.
- Saleh, A. and Fryrear D. W. 1995. Threshold wind velocities of wet soils as affected by wind blown sand. *Soil Science* 160(4):304-309.
- Saxton, K.E., Chandler, D., Stetler, L., Lamb, B., Claiborn, C. and Lee, B.H. 2000. Wind erosion and fugitive dust fluxes on agricultural lands in the Pacific Northwest. *Transactions of the American Society of Agricultural Engineers* 43(3):623-630.
- Schack, C.J., Pratsinis, S.E., and Friedlander, S.K. 1985. A general correlation for deposition on suspended particles from turbulent gases to completely rough surfaces. *Atmospheric Environment* 19(6): 953-960.

- Shao, Y., Raupach, M. and Leys, J.F. 1996. A model for predicting aeolian sand drift and dust entrainment on scales from paddock to region. *Australian Journal of Soil Research* 34:309-342.
- Skidmore, E.L. and Layton, J.B. 1992. Dry-soil aggregate stability as influenced by selected soil properties. *Soil Science Society of America Journal* 56(1):557-561.
- U.S. EPA. 1996. National ambient air quality standards for particulate matter: Proposed decision. 40 CFR 50 61(241), *Federal Register* 61(241).
- Van Dijk, P.M., Arens, S.M., and Van Boxel, J.H. 1999. Aeolian processes across transverse dunes. II. Modeling the sediment transport and profile development. *Earth Processes and Landforms* 24:319-333.
- Wagner, L.E. and Hagen, L.J. 1992. Relationship between shelter angle and surface roughness and cumulative sheltered storage depth. In: J. Karacsony and G. Szalai (eds.) *Proceedings of the International Wind Erosion Workshop of CIGR; September 10-12, 1991, Budapest, Hungary, V. Section I, 10 pp.*
- White, B.R. and Tsoar, H. 1998. Slope effect on saltation over a climbing sand dune. *Geomorphology* 22:159-180.
- Woodruff, N.P. and Siddoway, F.H. 1965. A wind erosion equation. *Soil Science Society of America Proceedings* 29(5):602-608.
- Zobeck, T.M. 1989. Fast-Vac a vacuum system to rapidly sample loose granular material. *Transactions of the American Society of Agricultural Engineers* 32(4):1316-1318.
- Zobeck, T.M. and Fryrear, D.W. 1986. Chemical and physical characteristics of windblown sediment I. Quantities and physical characteristics. *Transactions of the American Society of Agricultural Engineers* 29(4):1032-1036.
- Zobeck, T.M. and Onstad, C.A. 1987. Tillage and rainfall effects on random roughness: A review. *Soil & Tillage Research* 9:1-20.
- Zobeck, T.M. and Popham, T.W. 1992. Influence of microrelief, aggregate size, and precipitation of soil crust properties. *Transactions of the American Society of Agricultural Engineers* 35(2):487-492.

## Figure Captions

- Fig. 1. Example illustrating effects of three distributions of relative soil surface condition on average erosion when the relationship between erosion loss and surface condition is non-linear.
- Fig. 2. Static threshold friction velocity as a function of immobile clod and crust cover on bare, dry soil for a range of aerodynamic roughness with cover values less than 1.0.
- Fig. 3. Maximum soil discharge at wind speed of  $15 \text{ m s}^{-1}$  for saltation and creep compared to a range of suspension discharge rates corresponding to a range of visibilities at 1.83 m height.
- Fig. 4. Schematic of a control volume on a bare, rough, eroding surface illustrating friction velocity as the driving force and sources and sinks for saltation/creep (dashed lines) and suspension (solid lines) discharge.
- Fig. 5. Coefficient of abrasion of dry, immobile clods and crust as a function of natural logarithm of crushing energy ( Hagen et al., 1992).
- Fig. 6. Relative discharge below 1 m as a function of downwind distance for saltation/creep aggregates  $< 0.106 \text{ mm}$  and total aggregates  $< 0.050 \text{ mm}$  in diameter at Owens Lake, CA. The difference between the lines represents part of the suspension discharge (Gillette et al., 1997).
- Fig. 7. Ratio of PM<sub>2.5</sub>/PM<sub>10</sub> created by breakage of saltation-size aggregates as a function of the sand/clay ratio of the parent soil for sand  $> 0.1 \text{ mm}$  diameter (Hagen, 2001 b).

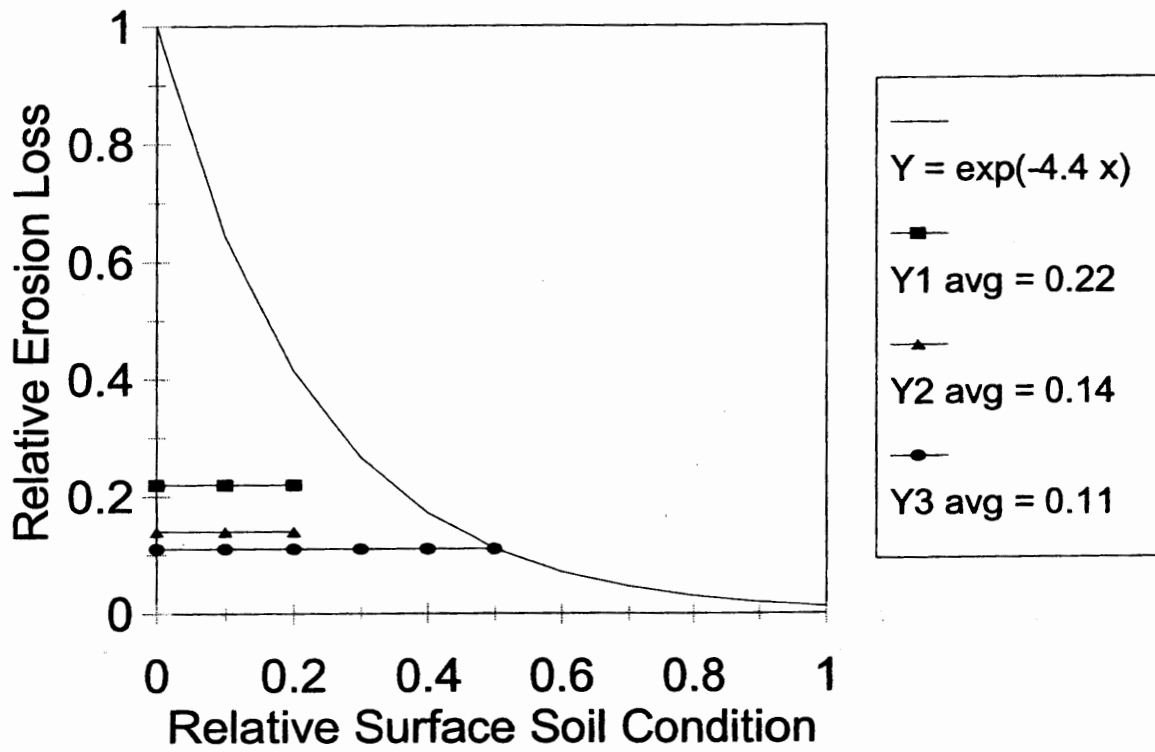


Fig. 1. Example illustrating effects of three distributions of relative soil surface condition on average erosion when the relationship between erosion loss and surface condition is non-linear.

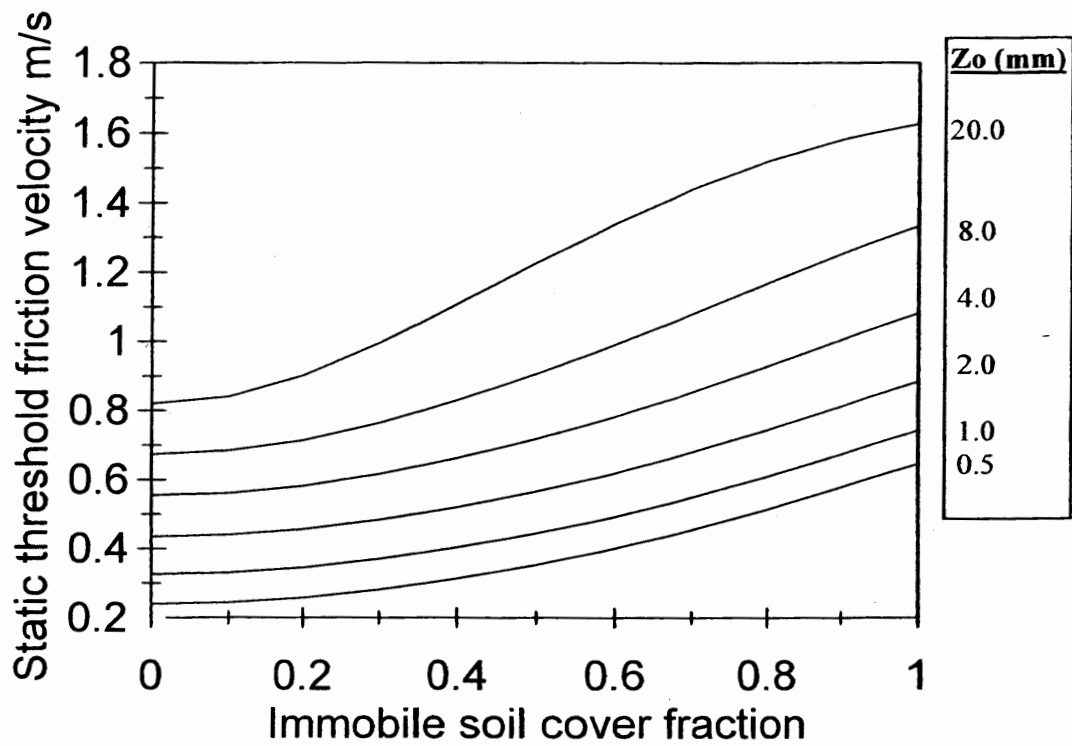


Fig. 2. Static threshold friction velocity as a function of immobile clod and crust cover on bare, dry soil for a range of aerodynamic roughness with cover values less than 1.0.

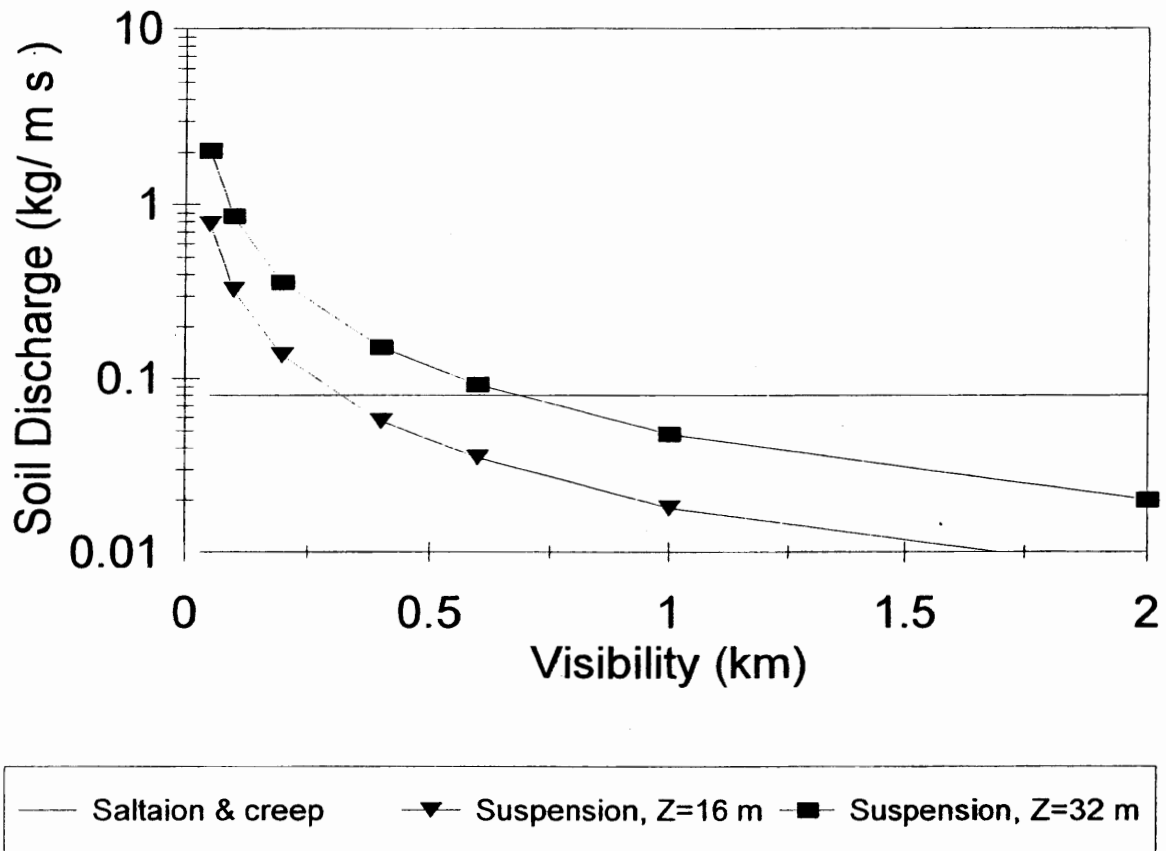


Fig. 3. Maximum soil discharge at wind speed of  $15 \text{ m s}^{-1}$  for saltation and creep compared to a range of suspension discharge rates corresponding to a range of visibilities at 1.83 m height.

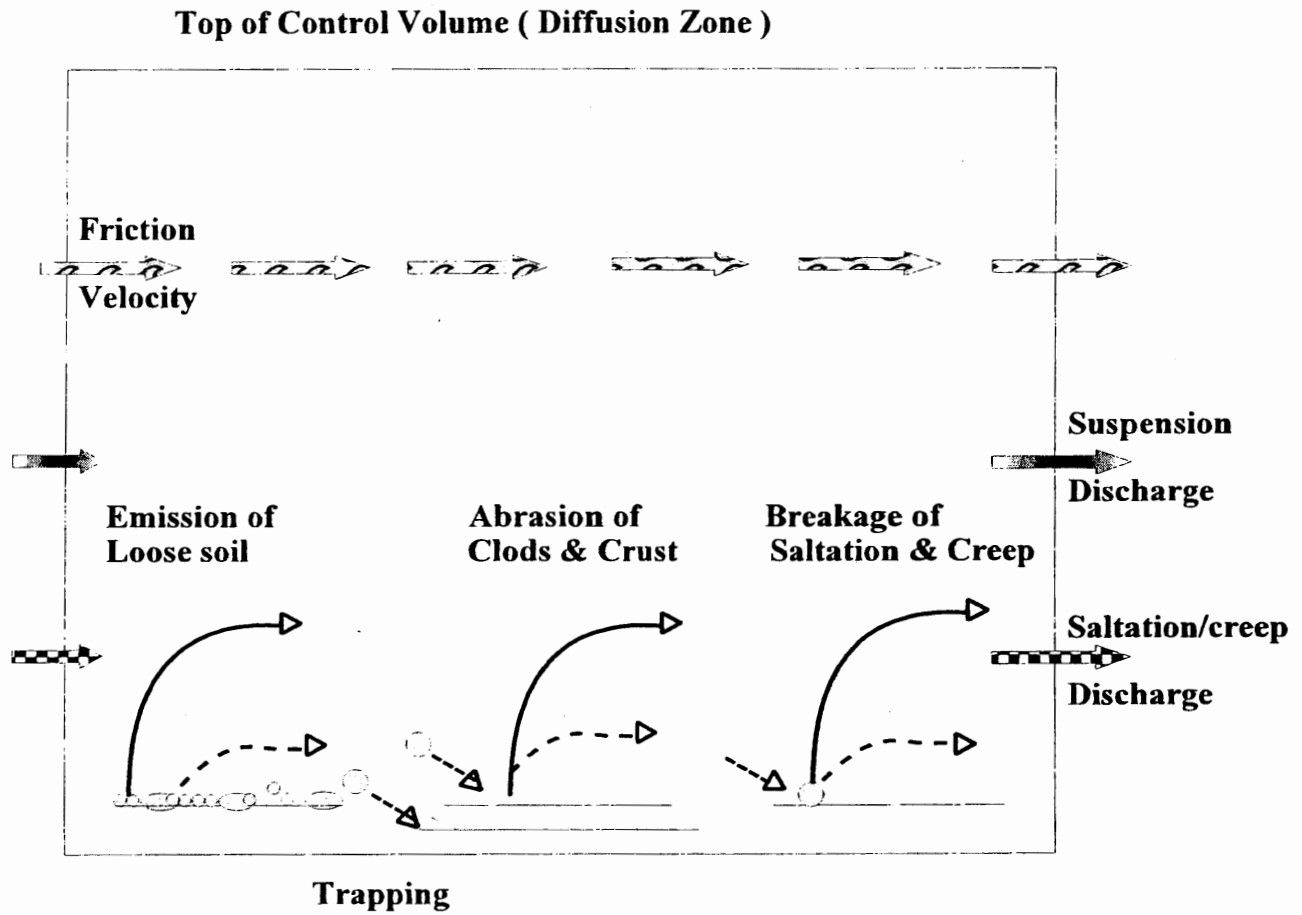


Fig. 4. Schematic of a control volume on a bare, rough, eroding surface illustrating friction velocity as the driving force and sources and sinks for saltation/creep (dashed lines) and suspension (solid lines) discharge.

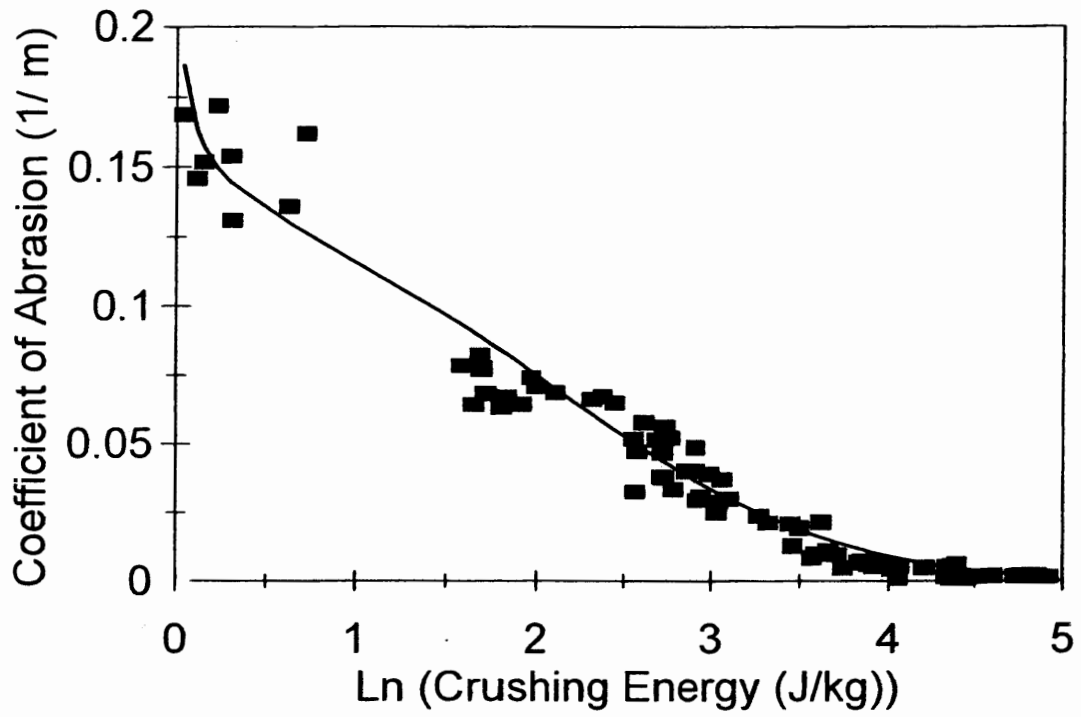


Fig. 5. Coefficient of abrasion of dry, immobile clods and crust as a function of natural logarithm of crushing energy ( Hagen et al., 1992).

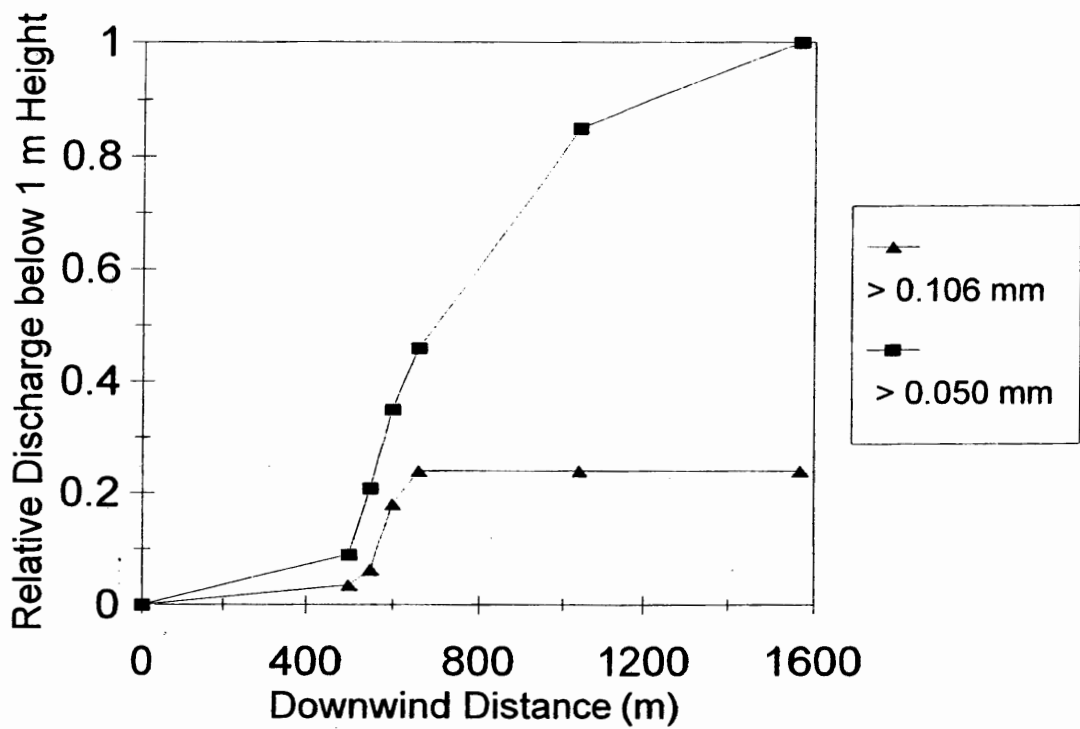


Fig. 6. Relative discharge below 1 m as a function of downwind distance for saltation/creep aggregates  $< 0.106$  mm and total aggregates  $< 0.050$  mm in diameter at Owens Lake, CA. The difference between the lines represents part of the suspension discharge (Gillette et al., 1997).

